In situ high-energy x-ray reflectivity studies of hydrophobic polyelectrolytes at the solid/liquid interface

2005 J. Phys.: Condens. Matter 17 6329

(http://iopscience.iop.org/0953-8984/17/41/004)

INSTITUTE OF PHYSICS PUBLISHING JOURNAL OF PHYSICS: CONDENSED MATTER

J. Phys.: Condens. Matter **17** (2005) 6329–6336 doi:10.1088/0953-8984/17/41/004

In situ high-energy x-ray reflectivity studies of hydrophobic polyelectrolytes at the solid/liquid interface

D Baigl[1,2], M Sferrazza[3,6], M-A Guedeau-Boudeville[1], R Ober[1], F Rieutord[4], O Théodoly[5] and C E Williams[1,7]

[1] Laboratoire de Physique des Fluides Organisés, CNRS UMR 7125, Collège de France, Paris, France
[2] Département de Chimie, CNRS UMR 8640, École Normale Supérieure, Paris, France
[3] Département de Physique, Université Libre de Bruxelles, Boulevard du Triomphe, CP223, Bruxelles, Belgium
[4] DRFMC-SI3M, CEA-Grenoble and ESRF BM32 beamline, Grenoble, France
[5] Complex Fluids Laboratory, CNRS/Rhodia UMR 166, Cranbury, NJ 08512, USA

E-mail: msferraz@ulb.ac.be

Received 10 March 2005, in final form 2 August 2005
Published 30 September 2005
Online at stacks.iop.org/JPhysCM/17/6329

Abstract

Well-defined hydrophobic polyelectrolytes adsorbed onto oppositely charged solid surfaces at the solid/liquid interface have been investigated. We have used *in situ* high-energy x-ray reflectivity to study how the thickness h of the adsorbed layer depends on the polymer effective charge fraction f_{eff} and on the chain length N. We have found $h \propto N f_{\text{eff}}^{-2/3}$, suggesting a pearl-necklace conformation for the chains in the adsorbed layer.

This article is dedicated to our colleague Claudine Williams.

1. Introduction

Polyelectrolytes are macromolecules containing ionizable groups which, in a polar solvent like water, dissociate into charges tied to the polymer backbone and counter-ions dispersed in the solution. They are called hydrophobic when water is a poor solvent for the backbone. As amphiphilic water-soluble macromolecules, hydrophobic polyelectrolytes are of great interest for industrial applications; in nature, many biological macromolecules, proteins for instance, have some intrinsic hydrophobicity. However, even if experiments [1–4], theories [5–7] and simulations [8, 9] are now all consistent with a pearl-necklace conformation for the single chain, the physics of hydrophobic polyelectrolytes is still far from being fully understood. Indeed,

[6] Author to whom any correspondence should be addressed.
[7] Deceased.

the role of counter-ions, the long-range electrostatic interactions, the short-range monomer–monomer interactions and solvent effects make simulations and theories difficult to achieve. On the experimental side, the combination of poor contrast in scattering experiments and fluctuations of concentration with a wide range of length scales (from a few nanometres for the pearl size up to a micron for the Debye length in pure water) make the interpretation of bulk properties in salt-free solutions rather delicate [10, 11]. Adsorbing chains onto solid surfaces could be an interesting way to freeze the fluctuations of concentration and eventually those of conformation [12].

In this work we have investigated model hydrophobic polyelectrolyte monolayers adsorbed onto oppositely charged or hydrophobic solid surfaces. Adsorbed layers were characterized *in situ*, in the aqueous solution at the solid–liquid interface, by the technique of x-ray reflectivity with high-energy photons. In a previous study, we have used *in situ* ellipsometry to investigate the properties of hydrophobic polyelectrolyte monolayers adsorbed onto oppositely charged solid surfaces. It has allowed us to establish the conditions for which the pearl-necklace conformation of the chains persisted upon adsorption. This required the presence of added salt in order for the Debye length to be comparable to the pearl size. In this case, the thickness of the adsorbed layer is proportional to the pearl size [13]. For the present study, the adsorbed layer was prepared with the same operating conditions (oppositely charged solid surface and presence of added salts) and we have measured the thickness and roughness of the adsorbed layer as a function of the chemical charge fraction and the length of the chains. In order to investigate the effect of the solvent quality, we have made a parallel study of the adsorption of a model hydrophilic polyelectrolyte. Finally, since hydrophobic polyelectrolytes are amphiphilic molecules [14], we present preliminary results for the adsorption onto neutral hydrophobic solid surfaces.

2. Experimental section

As a model hydrophobic polyelectrolyte we have used poly(styrene-*co*-styrenesulfonate, caesium salt) (PSS). This random copolymer is soluble in water when it contains more than 30% of styrenesulfonate monomers on average. A series of well-defined monodisperse PSSs of various chain lengths N and chemical charge fractions f, i.e., molar percentage of styrenesulfonate per chain, was synthesized and characterized according to a procedure described elsewhere [15]. Previous osmotic pressure and freezing point depression measurements have shown a strong reduction of the effective charge fraction f_{eff} as a function of f. We have found that f_{eff} obeys the following empirical renormalization law ($f \geqslant 18\%$) [1, 16]:

$$f_{\mathrm{eff}}(\%) = 100\frac{f - f^*}{100 - f^*}\frac{a}{l_{\mathrm{B}}} = \frac{f(\%) - 18}{82}36 \tag{1}$$

where f^* is the chemical charge fraction (18%) at which f_{eff} equals 0, a is the monomer size (0.25 nm) and l_{B} is the Bjerrum length (0.71 nm in pure water at 25 °C). The characteristics of PSS samples used in this study are summarized in table 1.

As a model hydrophilic polyelectrolyte we have used poly(acrylamide-*co*-acrylamidomethylpropanesulfonate, caesium salt) (AMAMPS) because its polyacrylamide backbone is water soluble. Here the chemical charge fraction f is the molar percentage of acrylamidomethylpropanesulfonate monomer per chain and it was measured by ^{1}H NMR (Bruker Avance300 spectrometer) in deuterium oxide (Aldrich). AMAMPSs with f ranging from 34% to 100% have been synthesized by radical copolymerization of acrylamide (Aldrich) and sodium 2-acrylamido-2-methyl-1-propanesulfonate [17].

Table 1. PSS samples of various chain lengths N, chemical charge fractions f (%) and effective charge fractions f_{eff} (%). f_{eff} is estimated from f using equation (1).

N	f	f_{eff}	N	f	f_{eff}	N	f	f_{eff}
930	33	6.6	1320	36	7.9	2520	37	8.3
930	41	10.1	1320	53	15.4	2520	54	15.8
930	46	12.3	1320	71	23.3	2520	89	31.2
930	53	15.4	1320	100	36.0			
930	62	19.3						
930	75	25						
930	83	28.5						

Two types of solid surfaces were prepared: (a) positively charged surface (PCS) and (b) neutral hydrophobic surface (HS). For this purpose, self-assembled monolayers (SAMs) were grafted on the native silica layers covering silicon wafers (Siltronix, Archamps, France; diameter: 25.4 mm, thickness: 2 mm) with the same procedure as described in [13]. The silica layer thickness h_{SiO_2} was measured by ellipsometry in air after activation and before silanation. The SAM thickness h_{SAM} was measured by ellipsometry in air while its roughness σ_{SAM} and density ρ_{SAM} were measured by x-ray reflectivity in air at our laboratory. The topography was checked by atomic force microscopy. All these measurements are consistent with a dense self-assembled monolayer ($h_{\text{SAM}} = 1.1$ nm for PCS and 0.4 nm for HS, $\rho_{\text{SAM}} = 0.29\ \text{e}^{-}\ \text{Å}^{-3}$, $\sigma_{\text{SAM}} = 0.5$ nm).

Polyelectrolyte layers were prepared by spontaneous adsorption from aqueous solution of polymer at 0.01 mol l^{-1} and CsCl at 0.1 mol l^{-1}. Under these conditions it has been shown that the pearl-necklace conformation persists in the adsorbed state [13, 18].

X-ray reflectivity experiments were performed on BM32 beamline of the European Synchrotron Radiation Facility (ESRF) in Grenoble (France) at a photon energy of 27 keV ($\lambda \approx 0.046$ nm) corresponding to a critical angle $\theta_{\text{c}} \approx 0.048°$ ($q_{\text{c}} \approx 0.23\ \text{nm}^{-1}$). A point, low-background scintillation detector was used. The high-precision beamline goniometer was used in the range $0° \leqslant \theta \leqslant 0.76°$ ($0 \leqslant q \leqslant 3.6\ \text{nm}^{-1}$). Working at such small angles requires perfectly planar surfaces. Hence, before each *in situ* reflectivity experiment, the planarity of the solid surface was checked by measuring the width of the reflected beam. The incident beam was limited by slits to a size of $l = 1$ mm (horizontal width) by $h = 20\ \mu$m (vertical height). The corresponding footprint at θ_{c} had a longitudinal length $L \approx 23.9$ mm, which is slightly smaller than the wafer size (25.4 mm). We used a custom-made liquid cell with a diameter of 26 mm, shown in figure 1. It is made of Kelev, a hydrophobic polymer material that prevents chemical and ionic contamination, with Kapton (non-absorbing material with negligible scattering) windows. The 2 mm thick solid surface was maintained by depression and the cell was flushed with the surface kept immersed. Under these conditions, the absorption coefficient was approximately $\alpha \approx 0.3$. The background for the reflectivity curve was measured at an angle of $2\theta + 0.1°$ and subtracted afterwards. It was checked that during the typical exposure time of about 15 min, no beam damage of the surface occurred.

3. Results and discussion

A typical *in situ* reflectivity R scan for a model hydrophobic polyelectrolyte layer (PSS, $N = 2520$, $f = 37\%$) immersed in water is presented in the inset of figure 2, where $\log(R)$ is plotted as a function of the vertical momentum transfer q. The critical edge at $q_{\text{c}} = 0.23\ \text{nm}^{-1}$ is clearly visible. For $q < q_{\text{c}}$, R is less than 1 for geometric reasons. For $q > q_{\text{c}}$, R decreases

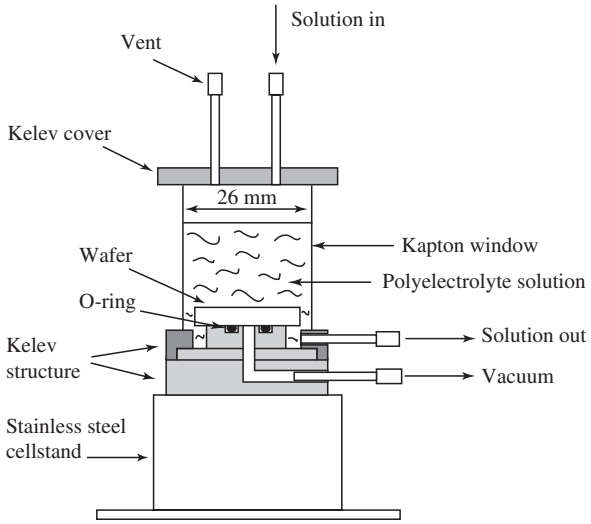

Figure 1. Liquid cell for the reflectivity experiment.

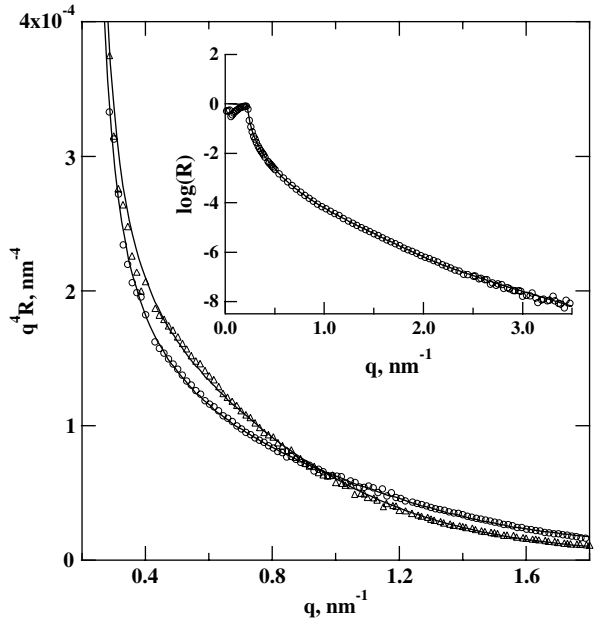

Figure 2. Typical reflectivity R scan as a function of the vertical momentum transfer q for an adsorbed PSS layer ($N = 2520$, $f = 37\%$) immersed in water. q^4R as a function of q before (open triangles) and after (open circles) the adsorption. Inset: $\log(R)$ as a function of q. Solid lines result from fits using Parratt's algorithm [23] and a Nevot and Croce's roughness [24].

steeply as a function of q. In the case of a sharp interface, the reflectivity (called also the Fresnel reflectivity R_F) will vary with q^{-4} at high values of q. Therefore $q^4 R_F(q)$ will be a constant. The presence of a diffuse interface will cause the scattering intensity to fall more rapidly than q^{-4} and the structure of the real interface can be extracted from a $q^4 R(q)$ versus

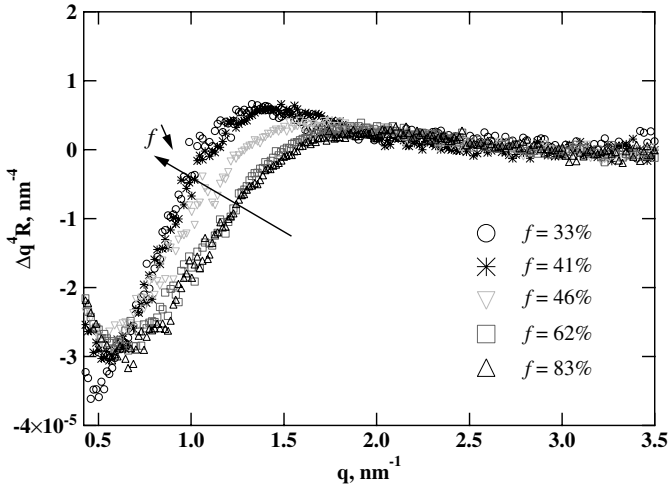

Figure 3. $\Delta q^4 R$ as a function of the vertical momentum transfer q for PSS of chain length $N = 930$ and various chemical charge fractions f. The arrow indicates decreasing values of f.

q plot. In the main graph of figure 2, $q^4 R$ is plotted as a function of q in a limited q-range for a PCS surface before (open triangles) and after (open circles) the adsorption of the PSS layer. In this representation, the presence of the PSS layer is clearly evidenced, the $q^4 R$ curve being first below, crossing at $q \approx 1\ \mathrm{nm}^{-1}$ and staying finally above that of the bare surface. To make the contribution of the PSS layer even more apparent, the difference between the scattering intensity after the adsorption (in the presence of the PSS layer) and before adsorption can be calculated. In particular the difference $\Delta q^4 R$ can be defined as follows:

$$\Delta q^4 R = q^4 R_{\text{after adsorption}} - q^4 R_{\text{before adsorption}} \tag{2}$$

where $R_{\text{after adsorption}}$ is the reflectivity after the adsorption and $R_{\text{before adsorption}}$ is the reflectivity, on the same sample, before the adsorption. The quantity $\Delta q^4 R$ was determined from the experimental data and is plotted in figure 3 as a function of q for a series of PSS of a chain length $N = 930$ and various chemical charge fractions f. It shows a strong dependence of $\Delta q^4 R$, i.e., of the layer characteristics, on f.

The same experiment was performed with the model hydrophilic polyelectrolyte called AMAMPS. Here the $\Delta q^4 R$ curves as a function of q for AMAMPS of various chemical charge fractions in the same range as those for PSS were superposable, indicating that the properties of the adsorbed AMAMPS layer are independent of f. These experiments show a clear difference in the adsorption behaviour of the hydrophilic polyelectrolytes and the hydrophobic ones. At this point, one should recall that the bulk solution properties of the same polymers are also markedly different. For AMAMPS, it has been shown that the structure of the solution is independent of f in the range where the effective charge fraction is renormalized by Manning condensation to a constant value of 36% [19]. In contrast, for PSS solutions, the structural characteristics all depend on f and corroborate the pearl-necklace conformation of the single chain [10, 11]. At the same time the effective charge has been found to be a strong function of f (see equation (1)). It is tempting to assume that the chain conformation at the surface is related to that in the bulk and that the evolution of the adsorbed PSS layer properties on f observed in figure 3 are related to conformational effects, i.e., the presence of pearls in the specific case of hydrophobic polyelectrolytes. Our system has been modelled as a stratified medium composed of two layers, SiO_2 and a polymer layer on a silicon substrate. The quality

Table 2. Properties of the PSS layers on oppositely charged surfaces extracted from the fits. N is the chain length, f (%) is chemical charge fractions, f_{eff} (%) is the effective charge fractions, h_{PSS} (nm) is the thickness, ρ_{PSS} (e^- Å^{-3}) is the electron density and σ_{PSS} (nm) is the roughness.

$N = 930$					$N = 1320$					$N = 2520$				
f	f_{eff}	h_{PSS}	ρ_{PSS}	σ_{PSS}	f	f_{eff}	h_{PSS}	ρ_{PSS}	σ_{PSS}	f	f_{eff}	h_{PSS}	ρ_{PSS}	σ_{PSS}
33	6.6	3.9	0.36	1.1	36	7.9	3.5	0.36	1.3	37	8.3	3.8	0.35	1.3
41	10.1	3.4	0.36	1.5	53	15.4	2.8	0.39	1.3	54	15.8	2.7	0.37	1.2
46	12.3	2.4	0.37	1.1	71	23.3	2.1	0.4	1.0					
53	15.4	2.2	0.38	1.1	100	36	1.4	0.39	0.9					
62	19.3	2.0	0.37	1.0										
75	25	1.9	0.38	0.9										
83	28.5	1.4	0.39	0.8										

Table 3. Properties of the PSS layers on hydrophobic surfaces extracted from the fits. N is the chain length, f (%) is chemical charge fractions, f_{eff} (%) is the effective charge fractions, h_{PSS} (nm) is the thickness, ρ_{PSS} (e^- Å^{-3}) is the electron density and σ_{PSS} (nm) is the roughness.

$N = 1320$				
f	f_{eff}	h_{PSS}	ρ_{PSS}	σ_{PSS}
36	7.9	3.1	0.42	0.9
53	15.4	2.7	0.35	0.9
71	23.3	2.2	0.35	0.9
100	36	1.1	0.36	0.9

of the fit of the experimental data is illustrated by the solid lines in figure 2. For all the data three fitting parameters were used: the PSS layer thickness h_{PSS}, its roughness σ_{PSS} and its electron density ρ_{PSS}. For each substrate, all other parameters have been fixed ($\rho_{\text{Si}} = 0.70$ e^- Å^{-3}, $\sigma_{\text{Si}} = 0.5$ nm, $\rho_{\text{SiO}_2} = 0.67$ e^- Å^{-3}, $\rho_{\text{H}_2\text{O}} = 0.33$ e^- Å^{-3}) or measured independently by ellipsometry (h_{SiO_2}) and *in situ* high-energy reflectivity prior to polyelectrolyte adsorption (h_{SAM}, ρ_{SAM}, σ_{SAM}). It is important to note that, whereas the thickness and roughness of the SAM inside water was found to be the same as that measured in air (by ellipsometry and x-ray reflectivity), its electron density systematically shifted from 0.29 e^- Å^{-3} in air to 0.45 e^- Å^{-3} in pure water[8]. Only this later value allowed us to fit the reflectivity profiles of the PSS layers, and it was used throughout. Each system was measured several times and the results from the fits are reported in table 2 for the PSS adsorbed on oppositely charged surfaces, and in table 3 for the PSS adsorbed onto hydrophobic surfaces. In tables 2 and 3, the electron density, the thickness and the roughness extracted from the fits are shown for the various systems measured.

The electron density ρ_{PSS} was found to increase as a function of f from 0.36 to 0.40 e^- Å^{-3}. This is to be expected since most of the contrast comes from the counter-ions in the layer. Indeed, according to the f_{eff} values (listed in table 1), the amount of condensed counter-ions per chain varies within a factor of 2 in the f range explored. Assuming that the adsorbed amount remains constant as verified by *in situ* ellipsometry [13], the electron density should increase accordingly. The roughness of the PSS layer has been measured to be between 1.0 and 1.5 nm, indicating the rough character of the adsorbed layer at a molecular level. This could be in qualitatively good agreement with the presence of pearls within the adsorbed PSS layer.

Figure 4 shows the measured thickness h_{PSS} of the PSS layers from tables 2 and 3 as a function of the effective charge fraction f_{eff}. Let us first consider the adsorption of PSS onto

[8] This anomalous increase was also observed in recent experiments on other interfaces in water [20, 21].

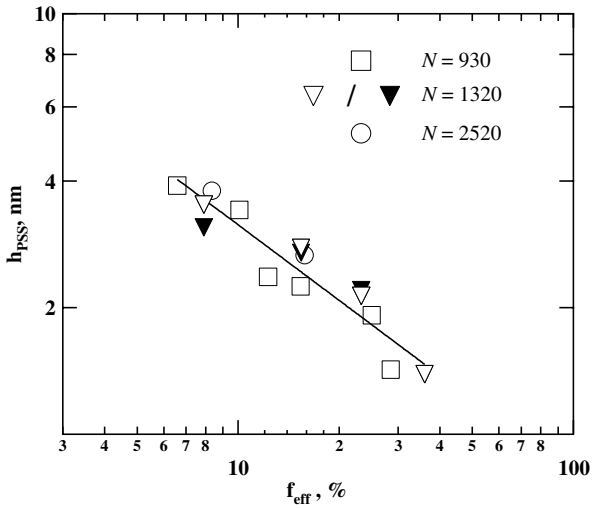

Figure 4. h_{PSS} of the adsorbed PSS layer as a function of the effective charge fraction f_{eff} for various chain lengths N. The straight line has a slope of $-2/3$. The open symbols correspond to the adsorption onto oppositely charged surfaces, the filled inverted triangles to the adsorption onto hydrophobic surfaces. Errors on experimental points are around 0.4 nm.

oppositely charged surfaces (open symbols). h_{PSS} decreases with f_{eff} and is independent of N. Since ρ_{PSS} and σ_{PSS} appear to be only slightly dependent on f, the strong evolution with f observed in figure 3 is mostly due to variations of h_{PSS}. Within experimental accuracy, the h_{PSS} dependence on f_{eff} is in agreement with the power law:

$$h_{PSS} \propto a N^0 f_{eff}^{-2/3} \tag{3}$$

as represented by the straight line in figure 4.

For all films, the thickness was the same in the adsorbing solution or after flushing with pure water, indicating that all adsorbed chains are strongly attached to the surface and do not desorb. On the other hand, the results of figure 4 and equation (3) are in perfect agreement with previous results from *in situ* ellipsometry experiments performed on the same system [13]. In contrast to ellipsometry, x-ray reflectivity does not require any assumption on the refractive index and allows one to establish the electron density profile. X-ray reflectivity is thus a reliable and accurate technique to fully characterize a polyelectrolyte monolayer at a solid–liquid interface. As has been shown experimentally [13], and predicted theoretically [18], the pearl-necklace conformation persists upon adsorption in these conditions of screened electrostatic attraction to the surface. Furthermore, the electrostatic repulsion between two neighbouring pearls is sufficiently screened to induce a compaction of the pearl-necklace on its pearls. Therefore, the PSS layer could be viewed as a dense carpet of pearls. The thickness h_{PSS} is closely related to the pearl size D_p and we could assume that h_{PSS} is proportional to D_p. In fact by analogy with the Rayleigh instability of a charged droplet, D_p is predicted [6] to scale as:

$$D_p \propto a N^0 \lambda^{-2/3} \tag{4}$$

where λ is the linear charge density along the chain. For a real polyelectrolyte system, we assume that λ is given by the effective charge fraction f_{eff} and we could expect that D_p scales as equation (3), as our data indicate. Moreover, our data confirm that the effective charge fraction f_{eff}, rather than f, is controlling the intra-chain electrostatic interactions.

All previous results dealt with the adsorption on positively charged surfaces (PCSs). We have to be concerned with the deformation of pearls upon adsorption since a strong flattening of pearls has also been predicted in the case of unscreened attraction [22]. For this purpose, we have also studied, in a less extended way, the adsorption of PSS onto hydrophobic surfaces (HSs). This corresponds to the filled symbols in figure 4. In this case the chains have to diffuse toward the HS and the adsorption process is slow. In order to measure the equilibrium thickness in the case of HS, h_{PSS} has been measured after a contact time of 24 h between the surface and the PSS solution. Data of figure 4 are preliminary results and only three points have been obtained. Nevertheless, within experimental accuracy, it seems that the behaviour on the HS is identical to that on the PCS. In other words, the pearl-necklace conformation seems to persist also upon adsorption onto hydrophobic surfaces. We are now pursuing this study and we expect that further experiments will elucidate this interesting point.

4. Conclusions

In conclusion, a model hydrophobic polyelectrolyte (PSS) of various chain lengths N and effective charge fractions f_{eff} has been adsorbed onto oppositely charged surfaces immersed in water. *In situ* high-energy x-ray reflectivity indicates that in the presence of an adequate amount of added salts, the thickness and electron density are a strong function of the charge fraction, in marked contrast to the case of a hydrophilic polyelectrolyte (AMAMPS) adsorbed in the same conditions. We have found $h_{\mathrm{PSS}} \propto aN^0 f_{\mathrm{eff}}^{-2/3}$ in agreement with the scaling prediction for the pearl size D_{p}.

References

[1] Baigl D 2003 *PhD Thesis* Paris VI, Paris, France
http://tel.ccsd.cnrs.fr/documents/archives0/00/00/36/20/tel-00003620-00/tel-00003620.pdf
[2] Lee M-J, Green M M, Mikěs F and Morawetz H 2002 *Macromolecules* **35** 4216
[3] Kiriy A, Gorodyska G, Minko S, Jaeger W, Štěpánek P and Stamm M 2002 *J. Am. Chem. Soc.* **124** 13454
[4] Kirwan L J, Papastavrou G and Borkovec M 2003 *Nano Lett.* **4** 149
[5] Kantor Y and Kardar M 1994 *Europhys. Lett.* **27** 643
[6] Dobrynin A V, Rubinstein M and Obukhov S P 1996 *Macromolecules* **29** 2974
[7] Dobrynin A V and Rubinstein M 1999 *Macromolecules* **32** 915
[8] Micka U, Holm C and Kremer K 1999 *Langmuir* **15** 4033
[9] Limbach H-J and Holm C 2003 *J. Phys. Chem.* B **107** 8041
[10] Baigl D, Ober R, Qu D, Fery A and Williams C E 2003 *Europhys. Lett.* **62** 588
[11] Qu D, Baigl D, Williams C E, Mohwald H and Fery A 2003 *Macromolecules* **36** 6878
[12] Limbach H-J, Holm C and Kremer K 2002 *Europhys. Lett.* **60** 566
[13] Baigl D, Sferrazza M and Williams C E 2003 *Europhys. Lett.* **62** 110
[14] Théodoly O, Ober R and Williams C E 2001 *Eur. Phys. J.* E **5** 51
[15] Baigl D, Seery T A P and Williams C E 2002 *Macromolecules* **35** 2318
[16] Essafi W, Lafuma F, Baigl D and Williams C E 2005 *Europhys. Lett.* at press
[17] McCormick C L and Chen G S 1982 *J. Polym. Sci.: Polym. Chem. Edn* **20** 817
[18] Dobrynin A V and Rubinstein M 2002 *Macromolecules* **35** 2754
[19] Essafi W, Lafuma F and Williams C E 1999 *Eur. Phys. J.* B **9** 261
[20] Doer A K, Tolan M, Schlomka J-P and Press W 2000 *Europhys. Lett.* **52** 330
[21] Schwended D, Hayashi T, Steitz R, Dahint R, Pipper J, Pertsin A and Grunze M 2003 *Langmuir* **19** 2284
[22] Borisov O V, Hakem F, Vilgis T A, Joanny J-F and Johner A 2001 *Eur. Phys. J.* E **6** 37
[23] Parratt L G 1954 *Phys. Rev.* **95** 359
[24] Nevot L and Croce P 1980 *Rev. Phys. Appl.* **15** 761